

Implications of the first neutral current data from SNO for Solar Neutrino Oscillation

Abhijit Bandyopadhyay^{a1}, Sandhya Choubey^{b2}, Srubabati Goswami^{c3}, D.P. Roy^{de4}

^aSaha Institute of Nuclear Physics, Bidhannagar, Kolkata 700 064, INDIA

^b Department of Physics and Astronomy, University of Southampton, Highfield, Southampton S017 1BJ, UK

^c Harish-Chandra Research Institute, Chhatnag Road, Jhusi, Allahabad - 211-019, INDIA

^dTata Institute of Fundamental Research, Homi Bhabha Road, Mumbai 400 005, INDIA

^ePhysics Department, University of California, Riverside, Ca 92521, USA

Abstract

We perform model independent and model dependent analyses of solar neutrino data including the neutral current event rate from SNO. The inclusion of the first SNO NC data in the model independent analysis determines the allowed ranges of 8B flux normalisation and the ν_e survival probability more precisely than what was possible from the SK and SNO CC combination. We perform global $\nu_e - \nu_{active}$ oscillation analyses of solar neutrino data using the NC rate instead of the SSM prediction for the 8B flux, in view of the large uncertainty in the latter. The LMA gives the best solution, while the LOW solution is also acceptable at the 99% C.L. level.

¹e-mail: abhi@theory.saha.ernet.in

²email: sandhya@hep.phys.soton.ac.uk

³e-mail: sruba@mri.ernet.in

⁴e-mail:dproy@theory.tifr.res.in

The neutral current results from the Sudbury Neutrino Observatory measures for the first time the total flux of 8B neutrinos coming from the Sun [1]. In a recent paper [2] we had examined the role of the anticipated NC data from SNO in enhancing our understanding of the solar neutrino problem. As was shown in [3] the SNO NC rate can be expressed in terms of SNO CC and SK elastic scattering rates as

$$R_{SNO}^{NC} = R_{SNO}^{CC} + (R_{SK}^{el} - R_{SNO}^{CC})/r, \quad (1)$$

where $r = \sigma_{\nu_\mu, \tau}^{NC}/\sigma_{\nu_e}^{CC+NC} \simeq 0.157$ for a threshold energy of 5 MeV (including the detector resolutions and the radiative corrections to $\nu - e$ scattering cross-sections). All the rates are defined with respect to the BBP2000 Standard Solar Model (SSM) [4]. We showed in [2] that because SNO has a greater sensitivity to the NC scattering rate as compared to SK, the SNO NC measurement will be more precise and hence incorporation of this can be more predictive than the SNO CC and SK combination. We took three representative NC rates – $R_{NC}^{SNO} = 0.8, 1.0$ and $1.2 (\pm 0.08)$ and showed that

1. For a general transition of ν_e into a mixture of active and sterile neutrinos the size of the sterile component can be better constrained than before.
2. For transition to a purely active neutrino the 8B neutrino flux normalisation and the survival probability P_{ee} are determined more precisely.
3. We had also performed global two flavour oscillation analysis of the solar neutrino data for the $\nu_e - \nu_{active}$ case, where instead of R_{SK} and R_{SNO}^{CC} we used the quantities R_{SK}^{el}/R_{SNO}^{NC} and $R_{SNO}^{CC}/R_{SNO}^{NC}$. These ratios are independent of the 8B flux normalisation and hence of the SSM uncertainty. We showed that use of these ratios can result in drastic reduction of the allowed parameter regions specially in the LOW-QVO area depending on the value of the NC rate.

We now have the actual experimental result

$$R_{SNO}^{NC} = 1.01 \pm 0.12 \quad (2)$$

while eq. (1) gives 1.05 ± 0.15 . Thus in 306 live days (577 days) the SNO NC measurement has achieved a precision, which is already better than that obtained from the SK and SNO CC combination. This paper follows closely the analysis that we have done in [2] but incorporating the actual data. In addition we also perform an alternative global analysis for $\nu_e - \nu_{active}$ oscillation by letting the 8B normalisation factor f_B vary freely, where the inclusion of $R_{SNO}^{NC} (= f_B)$ in the fit serves to control this parameter. As we shall see below the two methods of global analysis give very similar results.

In section 1 we discuss the constraints on the electron neutrino survival probability, the 8B normalisation factor f_B and the fraction of sterile component without assuming any particular model for the probabilities. In section 2 we perform the global analyses assuming two flavour $\nu_e - \nu_{active}$ oscillation.

1 Model Independent Analysis

For the general case of ν_e transition into a combination of ν_{active} (ν_a) and $\nu_{sterile}$ (ν_s) states one can write the SK, SNO CC and SNO NC rates as

$$R_{SK}^{el} = f_B P_{ee} + f_B r P_{ea}, \quad (3)$$

$$R_{SNO}^{CC} = f_B P_{ee}, \quad (4)$$

$$R_{SNO}^{NC} = f_B (P_{ee} + P_{ea}), \quad (5)$$

where P_{ee} and P_{ea} denote the probabilities folded with the detector response function [5] and averaged over energy. To extract a model independent bound on P_{ee} one has to ensure an equality of the response functions which amounts to slight adjustment of the SK threshold energy and the rate [5, 6]. Our approach is slightly different. We treat P_{ee} to be effectively energy independent. The thresholds of both SNO and SK are now 5 MeV and the SK spectrum data indicate a flat probability down to 5 MeV [7] which is corroborated by the SNO spectrum [8, 9]. Hence we consider this assumption as justified and expect the results to be insensitive to the differences in the response functions. A comparison of the current values R_{SNO}^{CC} with R_{SNO}^{NC} is shown in fig. 1. It constitutes a 5.3σ signal for transition to a state containing an active neutrino component or alternatively a 5.3σ signal against a pure sterile solution.

Next we consider the general case where ν_e goes to a mixed state $= \nu_a \sin \alpha + \nu_s \cos \alpha$. Then one can write $P_{ea} = \sin^2 \alpha (1 - P_{ee})$. Substituting this in the equations (3) and (5) and eliminating P_{ee} using equation (4) one gets the following set of equations for f_B and $\sin^2 \alpha$ [2]

$$\sin^2 \alpha (f_B - R_{SNO}^{CC}) = (R_{SK}^{el} - R_{SNC}^{CC})/r, \quad (6)$$

$$\sin^2 \alpha (f_B - R_{SNO}^{CC}) = R_{SNO}^{NC} - R_{SNO}^{CC}. \quad (7)$$

We treat $\sin^2 \alpha$ as a model parameter. And for different input values of $\sin^2 \alpha$ we determine the central value and the 1σ and 2σ ranges of f_B by taking a weighted average of the equations (6) and (7). The corresponding curves are presented in fig. 2. Combining the 2σ lower limit of f_B from this fit with the 2σ upper limit from the SSM (vertical lines) gives a lower limit of $\sin^2 \alpha > 0.45$ i.e. the probability of the active component is $> 45\%$. Note that there is no upper limit on this quantity - i.e. the data is perfectly compatible with ν_e transition into purely active neutrinos.

Assuming transition into purely active neutrinos ($P_{ea} = 1 - P_{ee}$) we show in fig. 3 the 1σ and 2σ contours in the $f_B - P_{ee}$ plane from the combinations SK+SNOCC and SK+SNOCC+SNONC. The inclusion of the NC rate narrows down the ranges of f_B and P_{ee} . The error in f_B after the inclusion of NC data is about half the size of the corresponding error from SSM as is seen from fig. 3.

2 Model dependent analysis

In this section we present the results of our χ^2 analysis of solar neutrino rates and SK spectrum data in the framework of two flavour oscillation of ν_e to an active flavour. We use

the standard techniques described in our earlier papers [10, 11] excepting for the fact that instead of the quantities R_{SK}^{el} and R_{SNO}^{CC} we now fit the ratios R_{SK}^{el}/R_{SNO}^{NC} and $R_{SNO}^{CC}/R_{SNO}^{NC}$. The 8B flux normalisation gets cancelled from these ratios and the analysis becomes independent of the large (16-20%) SSM uncertainty associated with this. Further details of this fitting method can be found in [2]. In Table 2 we present the best-fit parameters, χ^2_{min} and goodness of fit (GOF). The best-fit comes in the HIGH(LMA) region as before [11, 12]. However as is seen from fig. 4a the incorporation of the NC data narrows down the allowed regions, and in particular the LOW region becomes much smaller.

We have also performed an alternative χ^2 fit to the rates of Table 1 [1, 7, 13, 14] along with the SK spectra by keeping f_B as a free parameter. Even though we allow f_B to vary freely the NC data serves to control f_B within a range determined by its error. As we see from Table 2 and fig. 4b the results of this fit are very similar to the previous case. The best fit comes from the HIGH(LMA) region, while a small LOW region is also allowed at the 99% CL level. Maximal mixing is seen to be just disallowed at the 3σ level even in the LOW region. To illustrate the impact of the NC rate on the oscillation solutions we have repeated the free f_B fit without this rate. The results are shown in fig 4c. Evidently the NC data plays a pivotal role in constraining the oscillation solutions, particularly in the LOW/QVO region.

3 Summary and Conclusions

The first SNO NC data constitutes a 5.3σ signal for transition into a state containing an active neutrino component. The inclusion of this data puts much tighter constraints on f_B and P_{ee} from a model independent analysis involving active neutrinos as compared to the SNO CC/SK combination. In this paper we have discussed two useful strategies, of incorporating the NC data in the global χ^2 analysis of rates and spectrum data, by which one can avoid the large 8B flux uncertainty from the SSM.

- We fit the ratios of the SK elastic and SNO CC rates w.r.t the NC rate, from which the f_B cancels out.
- We fit the rates by keeping f_B as a free parameter, where the inclusion of the SNO NC rate ($= f_B$) serves to control this parameter.

Both the analyses give very similar results. They clearly favour the HIGH(LMA) solution, while a limited region of the LOW solution is also acceptable at the 99% CL level. The maximal mixing solution is disfavoured at the 3σ level. As more data accumulate one expects a substantial reduction in the error bar of the SNO NC rate, resulting in further tightening of the allowed regions of neutrino mass and mixing.

Note Added: The paper [15] appeared on the net after completion of our work. In the region of overlap our results agree with theirs as well as with the updated version of [16]. The allowed LOW region of [9] is even smaller than ours presumably because they have included the error correlation between their NC and CC data. It may be added here that the SNO CC and NC rates given in Table 1 are obtained assuming undistorted energy spectra above 5 MeV, which has good empirical justification as mentioned above. We thank Prof. Mark Chen of SNO collaboration for communication on these points.

References

- [1] The SNO Collaboration (Q.R. Ahmad *et al.*), (submitted to Phys. Rev. Lett.), nucl-ex/0204008.
- [2] A. Bandyopadhyay, S. Choubey, S. Goswami and D.P. Roy, hep-ph/0203169.
- [3] V. Barger, D. Marfatia and K. Whisnant, Phys. Rev. Lett. **88**, 011302 (2002).
- [4] J.N. Bahcall, M.H. Pinsonneault and S. Basu, Astrophys. J. **555**, 990 (2001).
- [5] F.L. Villante, G. Fiorentini and E. Lisi, Phys. Rev. **D59**, 013006 (1999).
- [6] G.L. Fogli, E. Lisi, D. Montanino and A. Palazzo, Phys. Rev. **D64**, 093007 (2001).
- [7] S. Fukuda *et al.*, Super-Kamiokande collaboration, Phys. Rev. Lett. **86**, 5651 (2001).
- [8] The SNO Collaboration (Q.R. Ahmad *et al.*), Phys. Rev. Lett. **87**, 071301 (2001)
- [9] The SNO Collaboration (Q.R. Ahmad *et al.*), (submitted to Phys. Rev. Lett.), nucl-ex/0204009.
- [10] S. Goswami, D. Majumdar, A. Raychaudhuri, Phys. Rev. **D63**, 013003 (2001); *ibid* hep-ph/9909453. S. Choubey, S. Goswami, N. Gupta and D.P. Roy, Phys. Rev. **D64**, 053002 (2001);
- [11] A. Bandyopadhyay, S. Choubey, S. Goswami and K. Kar, Phys. Lett. **B519**, 83 (2001); S. Choubey, S. Goswami, K. Kar, H.M. Antia and S.M. Chitre, Phys. Rev. **D64**, 113001 (2001); S. Choubey, S. Goswami and D.P. Roy, Phys. Rev. **D65**, 073001 (2002); A. Bandyopadhyay, S. Choubey, S. Goswami and K. Kar, Phys. Rev. **D65**, 073031 (2002).
- [12] G.L. Fogli, E. Lisi, D. Montanino, A. Palazzo, Phys. Rev. **D64**, 093007 (2001); J.N. Bahcall, M.C. Gonzalez-Garcia, C. Pana-Garay, JHEP **0108**, 014 (2001); P.I. Krastev and A.Yu. Smirnov, e-Print Archive: hep-ph/0108177; M.V. Garzelli and C. Giunti, JHEP **0112**, 017 (2001).
- [13] J. N. Abdurashitov *et al.*, SAGE collaboration, Phys. Rev. **C 60**, 055801 (1999); W. Hampel *et al.*, GALLEX collaboration, Phys. Lett. **B447**, 127 (1999); M. Altman *et al.*, GNO collaboration, Phys. Lett. **B490**, 16 (2000).
- [14] B. Cleveland *et al.*, Ap. J. **496**, 505 (1998),
- [15] V. Barger, D. Marfatia, K. Whisnant and B.P. Wood, hep-ph/0204253.
- [16] P. Creminelli, G. Signorelli and A. Strumia, hep-ph/0102234 (updated version 3).

experiment	R	composition
Ga	0.584 ± 0.039	$pp(55\%), Be(25\%), B(10\%)$
Cl	0.335 ± 0.029	$B(75\%), Be(15\%)$
SK	0.459 ± 0.017 (0.358 ± 0.017)	$B(100\%)$
$SNO(CC)$	0.349 ± 0.021	$B(100\%)$
$SNO(NC)$	1.008 ± 0.123	$B(100\%)$

Table 1: The observed solar neutrino rates relative to the SSM predictions (BP2000) are shown along with their compositions for different experiments. For the SK experiment the ν_e contribution to the rate R is shown in parentheses assuming $\nu_e \rightarrow \nu_a$ transition.

Data Used	Nature of Solution	Δm^2 in eV 2	$\tan^2 \theta$	χ^2_{min}	Goodness of fit
$Ga +$	LMA	9.65×10^{-5}	0.39	30.85	78.82%
$SK/NC +$	LOW	1.34×10^{-7}	0.71	38.29	45.63%
$CC/NC +$	VO	4.34×10^{-10}	1.0	46.07	17.30%
SKspec	SMA	6.01×10^{-6}	1.66×10^{-3}	51.55	7.01%
$Cl + Ga +$	LMA	4.00×10^{-5}	0.38	33.77	70.69%
$SK + CC +$	LOW	1.19×10^{-7}	0.72	41.37	36.76%
$NC + SKspec$ + f_B free	VO	4.44×10^{-10}	1.22	47.59	16.27%
	SMA	6.03×10^{-6}	1.58×10^{-3}	57.71	2.72%

Table 2: The χ^2_{min} , the goodness of fit and the best-fit values of the oscillation parameters obtained for the analysis of the global solar neutrino data.

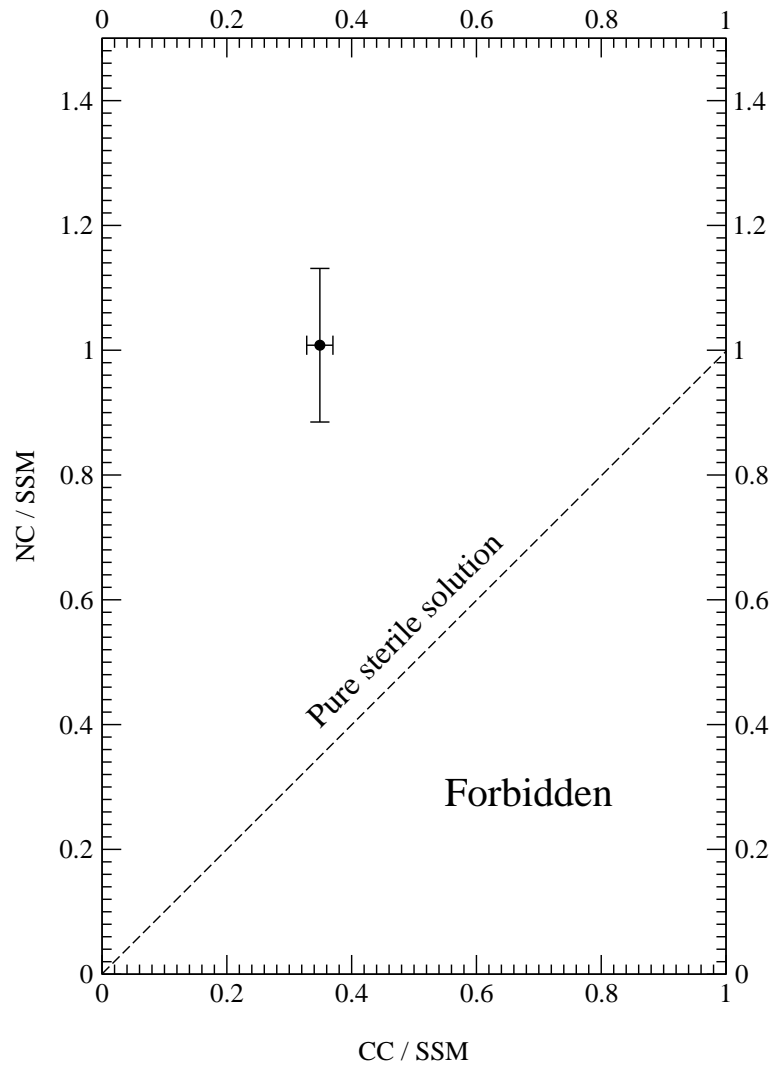


Figure 1: The SNO CC and NC rates shown relative to their SSM predictions. The dashed line is the prediction of the pure ν_e to ν_s transition. The pure sterile solution is seen to be disfavored at 5.3σ .

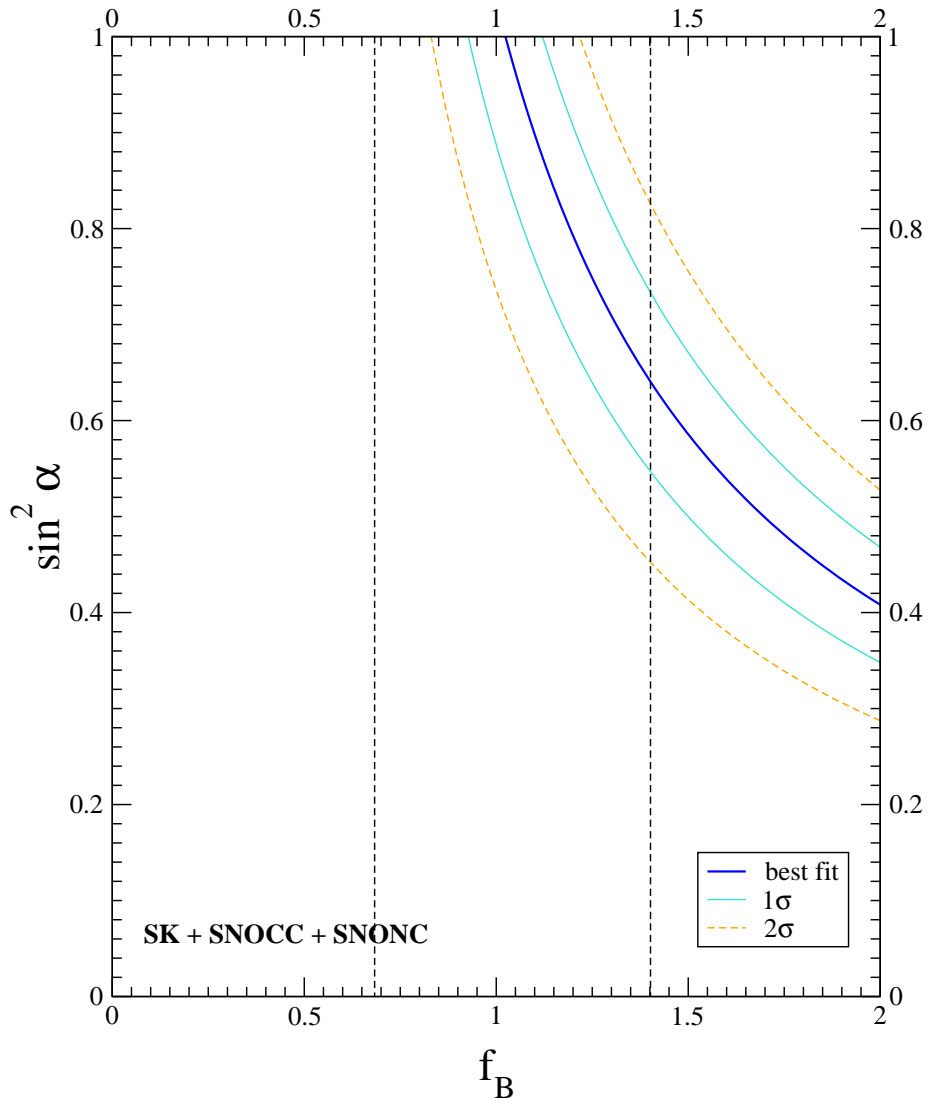


Figure 2: Best fit value of the 8B neutrino flux f_B shown along with its 1σ and 2σ limits against the model parameter $\sin^2 \alpha$, representing ν_e transition into a mixed state ($\nu_a \sin \alpha + \nu_s \cos \alpha$). The dashed line denote the $\pm 2\sigma$ limits of the SSM .

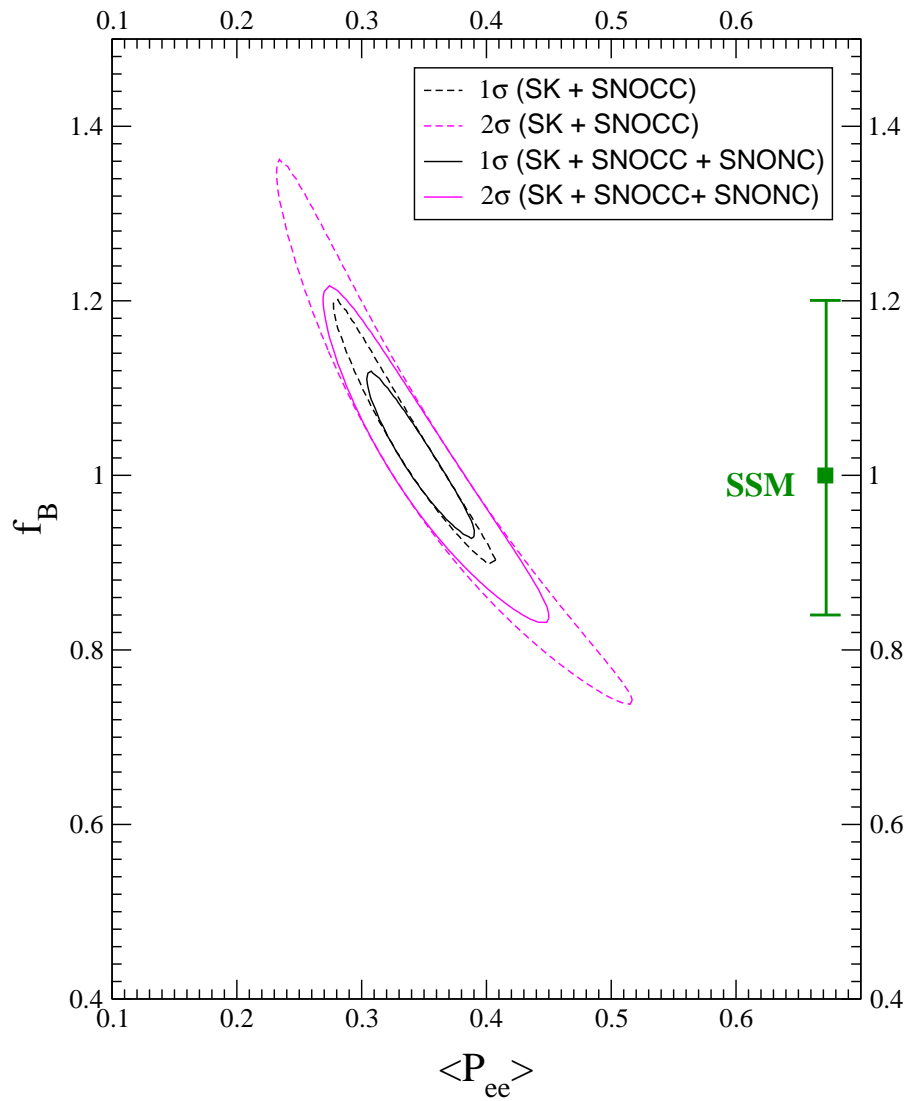


Figure 3: The 1σ and 2σ contours of solutions to the 8B neutrino flux f_B and the ν_e survival probability P_{ee} assuming ν_e to ν_a transition. The 1σ SSM error bar for f_B is indicated on the right.

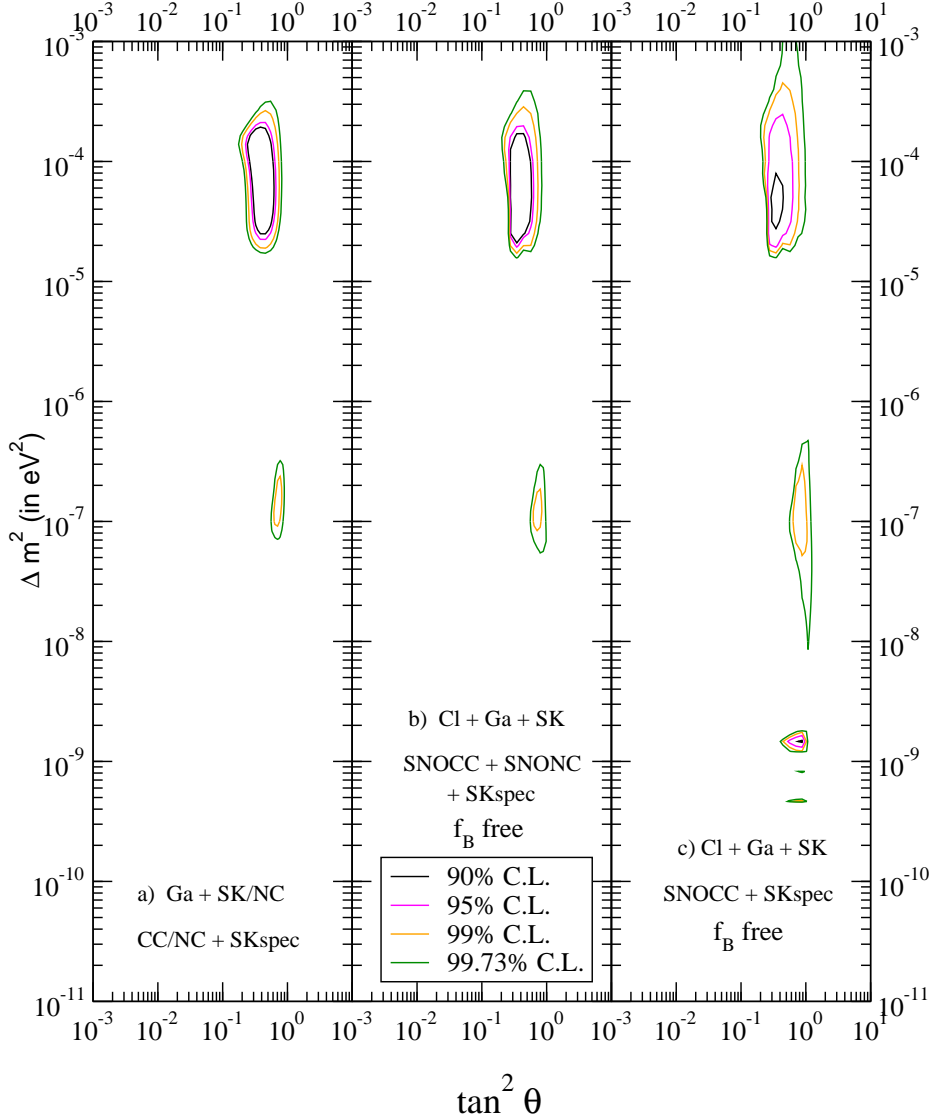


Figure 4: The $\nu_e \rightarrow \nu_a$ oscillation solutions to the global solar neutrino data using (a) Ga rate, the SK day-night energy spectra and the SK and $SNO(CC)$ rates, both normalised to the $SNO(NC)$ rate and (b) total Ga , Cl , SK , $SNO(CC)$ and $SNO(NC)$ rates along with the SK day-night energy spectra, keeping the 8B flux normalisation f_B free. In both cases we use the $SNO(NC)$ error as the error in the 8B flux. The case(c) is similar to (b), but without using the $SNO(NC)$ rate.